

High-power mid-infrared femtosecond fiber laser in the water vapor transmission window

SERGEI ANTIPOV,^{1,2} DARREN D. HUDSON,^{1,*} ALEXANDER FUERBACH,^{1,2} AND STUART D. JACKSON^{3,4}

¹MQ Photonics Research Centre, Department of Physics and Astronomy, Macquarie University, North Ryde, NSW 2109, Australia

²Centre for Ultrahigh bandwidth Devices for Optical Systems (CUDOS), Macquarie University, North Ryde, NSW 2109, Australia

³MQ Photonics Research Centre, Department of Engineering, Macquarie University, North Ryde, NSW 2109, Australia

⁴e-mail: stuart.jackson@mq.edu.au

*Corresponding author: darren.hudson@mq.edu.au

Received 7 September 2016; revised 18 October 2016; accepted 24 October 2016 (Doc. ID 275319); published 15 November 2016

The recent demonstrations of ultrafast mid-infrared fiber lasers emitting sub-picosecond pulses at 2.8 μm have created an exciting potential for a range of applications including mid-infrared frequency combs and materials processing. So far, this new class of laser has been based on the $^4\text{I}_{11/2}$ - $^4\text{I}_{13/2}$ transition in erbium-doped fluoride fibers, which lies directly in a region of high water vapor absorption. This absorption has limited the achievable bandwidth, pulse duration, and peak power and poses a serious problem for transmission in free space. In this Letter, we present an ultrafast mid-infrared fiber laser that overcomes these limitations by using holmium as the gain medium. Holmium allows the central emission wavelength to shift to nearly 2.9 μm and avoid the strong water vapor lines. This laser, which represents the longest wavelength mode-locked fiber laser, emits 7.6 nJ pulses at 180 fs duration, with a record peak power of 37 kW. At this power level, the laser surpasses many commercial free-space OPA systems and becomes attractive for laser surgery of human tissue, for industrial materials modification, and for driving broadband coherent supercontinuum in the mid-infrared. © 2016 Optical Society of America

OCIS codes: (060.2390) Fiber optics, infrared; (320.7090) Ultrafast lasers; (160.5690) Rare-earth-doped materials; (140.4050) Mode-locked lasers.

<http://dx.doi.org/10.1364/OPTICA.3.001373>

The recent creation of ultrashort-pulse fiber lasers operating in the 2.8 μm range [1–3] demonstrated that mode locking at wavelengths beyond the transmission window of silica fiber can be achieved with sub-picosecond performance. Traditionally, ultrashort pulses in the mid-infrared have been generated either through wavelength conversion of near-infrared mode-locked lasers in conjunction with nonlinear crystals [4], based on free-space solid-state *vibronic* lasers such as Cr:ZnSe/S [5], or with microresonator-based Kerr combs [6]. While the performance of these systems has reached a high level, their complexity has prevented widespread implementation across the fields of science

and industry in which they could have a high impact. Thus, the mid-infrared ultrafast fiber laser represents an exciting alternative: a laser with sub-picosecond pulses, multi-kilowatt-level peak power, diffraction-limited beam quality, and a robust fiber-based optical cavity that operates at room temperature. Indeed, this new class of laser could find application in a wide range of fields including breath analysis [7], molecular spectroscopy [8], and laser surgery of human tissue [9].

While the performance of mid-infrared ultrafast fiber lasers [10] continues to improve, intra-cavity molecular absorption in the free-space regions of the laser cavity remains problematic. Since important in-fiber components (e.g., splitters, wave-division multiplexors, waveplates) do not yet exist in this wavelength range, a portion of the cavity path contains an unavoidable free-space section. The most significant intra-cavity molecular absorption for lasers operating at 2.8 μm is due to water vapor. These strong water vapor absorption lines can limit the ultimate pulse bandwidth [1] or inhibit self-starting of the mode-locked laser [3]. In this work, we show that by using a holmium-doped ZrF₄-BrF₂-LaF₃-AlF₃-NaF (ZBLAN) fiber, which has an approximately 100 nm red-shifted emission wavelength compared to erbium-doped ZBLAN, we can generate 180 fs pulses, via nonlinear polarization rotation (NPR) mode locking. The holmium laser emission at 2876 nm is beyond the main water vapor lines (see Fig. 1), thereby mitigating the deleterious effects of intra-cavity water vapor absorption. Furthermore, the longer emission wavelength aligns better with the *liquid* water absorption peak, thus making this laser a potentially more attractive solution for human tissue surgery. The laser presented here represents, to the best of our knowledge, the first ultrafast mode-locked fiber laser that uses the holmium ion [11] and the longest wavelength ultrashort-pulse fiber laser to date.

Due to the cost and performance of commercial pump diodes, most of the efforts in mid-infrared fiber laser research have concentrated on erbium-doped ZBLAN [12]. In essence, this gain medium can be pumped by the same 980 nm diodes that were developed for the telecommunications industry, and the Stokes limit can be exceeded as a result of access to energy recycling via energy transfer upconversion [13]. To achieve mid-infrared emission in holmium, however, one needs to excite the $^5\text{I}_6$ - $^5\text{I}_7$

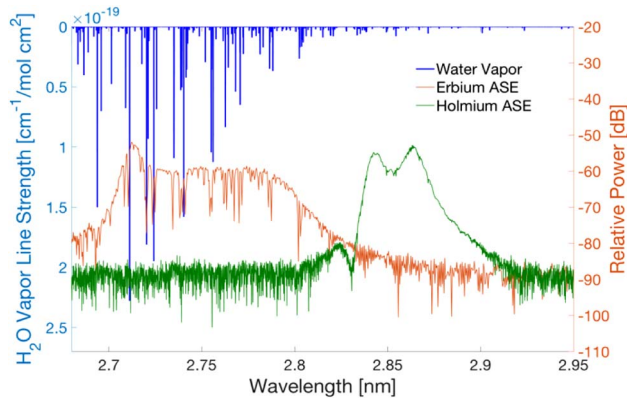


Fig. 1. Water vapor absorption lines (blue) overlaid with the amplified spontaneous emission (ASE) spectra of erbium-doped ZBLAN (orange) and holmium-doped ZBLAN (green). The effect of water absorption is drastically reduced despite the fact that the central emission wavelength from Ho^{3+} is only ~ 100 nm longer than Er^{3+} .

transition using 1150 nm pump photons. Traditionally, high-power diode sources have not been available at this wavelength. However, recent efforts in highly strained GaAs/InGaAs quantum well diodes and high-power Raman lasers based on Yb fiber lasers [14] have shown high performance (>100 W output) and robustness. In the current experiment, we polarization multiplex two commercial (Eagleyard Photonics) 4 W, multi-mode, 1150 nm diodes [15] to achieve up to 8 W of available pump power. Using these diodes, we reach pump power levels comparable to recent demonstrations of ultrafast mid-infrared fiber lasers based on erbium.

A slight complication of the use of holmium as a gain medium is its relatively long lower laser level lifetime—a situation that also applies to erbium-doped systems and that follows from the well-known increase in the rate of spontaneous emission with an increase in the energy of the initial level of the rare-earth ion laser transition. In holmium, the $^5\text{I}_7$ lifetime ($\tau_{\text{lower}} = 12.5$ ms) is longer than the $^5\text{I}_6$ upper laser lifetime ($\tau_{\text{upper}} = 3.5$ ms), which causes the transition to be self-terminating [16]. To overcome this, we have co-doped our fiber with a small amount of praseodymium, which is present at a level of 2500 ppm molar, and serves to desensitize the holmium lower laser level and force a straightforward four-level laser system. Through a highly resonant energy transfer process [16], the praseodymium ion reduces the holmium lower laser level lifetime to microsecond durations, allowing efficient lasing on this transition. As shown in Fig. 2, we launched the pump light through a dichroic mirror and into the pump cladding of a double-clad Ho^{3+} , Pr^{3+} -doped ZBLAN fiber (Fiberlabs Inc.). The fiber was 3.5 m long and had a mode field diameter of $14 \mu\text{m}$, a pump cladding diameter of $125 \mu\text{m}$, and an NA of 0.17. Via a full-wave numerical model, we calculated a group-velocity dispersion of $\beta_2 = -0.11 \text{ ps}^2/\text{m}$, and a nonlinear parameter (γ) of $3 \times 10^{-4} \text{ W}^{-1} \text{ m}^{-1}$. As in our earlier work with erbium [1], we performed angle cleaves on the end tips of the fiber to suppress feedback. Splicing multi-mode AlF_3 fiber also serves to suppress feedback from the fiber tips while protecting the fiber end face from contamination. The NPR method for mode locking was employed for this initial demonstration as the current performance of saturable absorbers in this wavelength region has not produced sub-picosecond pulses

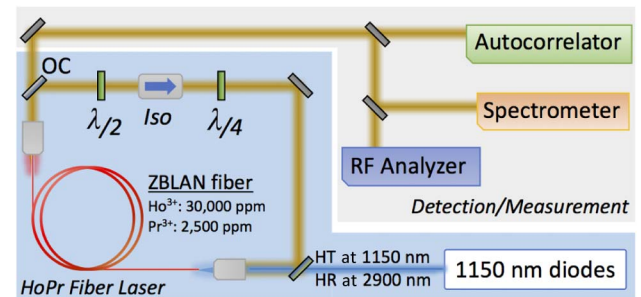


Fig. 2. Layout of the fiber laser cavity in which the NPR technique is used as the mode-locking mechanism. The output coupler (OC) had a transmission of 43%. The cavity consists of 3.5 m of fiber and 1.6 m of free space. The detection setup characterized the RF spectrum, optical spectrum, and pulse duration.

from an oscillator. Experimentally, NPR was achieved using one quarter-waveplate and one half-waveplate in conjunction with an isolator (Lasermetrics) in a free-space section of the cavity as shown in Fig. 2. Pulse selection by NPR was realized via the isolator's input polarizer. The isolator also served to stabilize the cavity against backreflections and ensure uni-directional operation. The output coupler was a dichroic mirror with 57% reflection and 43% transmission when angled at 45° . Once the correct mode-locked polarization setting was determined, the laser exhibited consistent self-starting behavior. Upon exiting the laser cavity, the pulse train was directed toward a suite of measurement devices including an interferometric autocorrelator, a mid-infrared spectrometer, and a fast photodetector (<2 ns rise time) that was combined with an RF analyzer or an oscilloscope. At a launched pump power of 3.2 W (launch efficiency = 80%), a 43.1 MHz pulse train appeared on the oscilloscope. Using the RF analyzer, we observed a fundamental beat with a signal-to-noise ratio (SNR) of >70 dB (RBW = 1 kHz), indicating a very stable pulse train. Furthermore, the harmonic beats showed an intensity roll-off in accordance with the bandwidth of our photodetector (Fig. 3). Using a Thorlabs OSA205 FTIR system, we recorded the optical spectrum shown in Fig. 4(a). Unlike the erbium system presented in [1], the mode-locked spectrum showed no signs of atmospheric absorption. The root-mean-square (rms) spectral

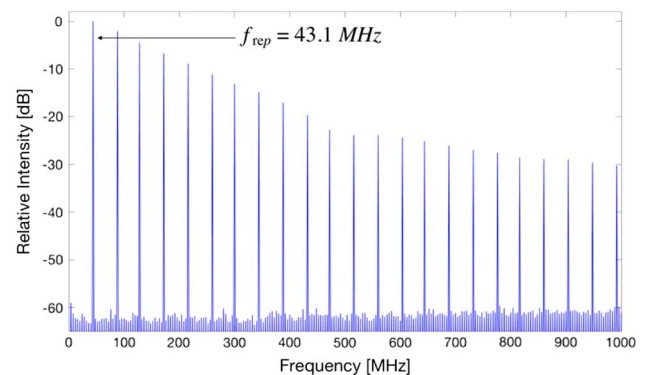


Fig. 3. Radio frequency spectrum from the fast photodiode. The fundamental repetition frequency of the laser is 43.1 MHz. The fundamental beat has a high SNR, indicating stable mode locking. The harmonic beats show a reduced intensity profile due to the finite photodetector bandwidth.

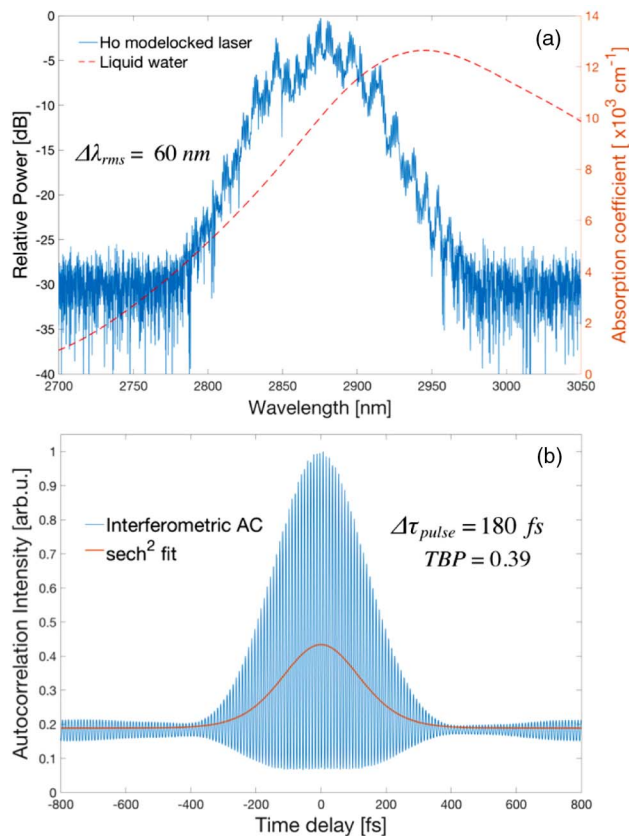


Fig. 4. (a) Optical spectrum of the mode-locked laser. The spectral centroid is 2876 nm, and the rms bandwidth is calculated to be 60 nm. The liquid water absorption (dashed line) peak is less than 70 nm away from the laser's spectral center. (b) Interferometric autocorrelation of the pulses. Assuming a sech^2 pulse shape, the actual pulse-width is 180 fs. The time-bandwidth product calculated from these two measurements is 0.39, which is 1.2 times the bandwidth limit.

bandwidth during mode locking was 60 nm, which is roughly three times the bandwidth achieved in the original erbium system [1] and two times that achieved in an optimized erbium-based cavity [3].

To measure the pulse duration, we used an interferometric autocorrelation technique. The results of this autocorrelation are shown in Fig. 4(b). As the dispersion of the fluoride fiber used in these experiments is anomalous at the emission wavelength, we expect soliton-based mode locking with sech^2 pulse shapes. Due to the soliton dynamics of self-phase modulation balancing the group-velocity dispersion of the cavity, the pulse should have very little chirp and be close to the transform limit given by the spectral bandwidth. At a central wavelength of 2876 nm, a single optical cycle is 9.59 fs in duration. As can be seen in Fig. 4(b), we have around 29 optical cycles within the FWHM of the autocorrelation signal. Taking into account the factor of 1.54 that the autocorrelation introduces, we calculate a pulsewidth of 180 fs, which is the shortest pulse reported to date in this class of fiber laser. Given that our spectrum has an rms bandwidth of 60 nm, the transform-limited pulsewidth is 145 fs. The slightly longer pulse that we observe is believed to be due to residual third-order spectral phase that is imparted by the fiber. The time-bandwidth product of this laser pulse is 0.39, or 1.2 times the fundamental limit of 0.315. Furthermore, the rms bandwidth of the ASE

spectrum of holmium (see Fig. 1) is ~ 120 nm. With an appropriate cavity dispersion map, this bandwidth could be achieved in a mode-locked laser, yielding a pulse duration directly from the oscillator of ~ 70 fs. One potential route to achieve this sub-100-fs performance is to use tailored fiber Bragg gratings to control the intra-cavity dispersion [17].

Given that the laser pulses obey soliton dynamics in the laser cavity, we expect that these shorter pulses should contain more energy than previous attempts according to the soliton area theorem. Indeed, we measure an average power of 327 mW (at a launched pump power of 3.2 W) for the pulse train, which corresponds to 7.6 nJ per pulse (in agreement with the theoretically predicted average intra-cavity soliton energy [18]). As has been noted previously [1,2], mid-infrared soliton lasers benefit from the reduced nonlinear parameter (γ) relative to their near-infrared counterparts. In fact, the pulse energy of a soliton laser in the mid-infrared can be more than an order of magnitude higher than that achievable in the near-infrared. This large pulse energy and short pulse duration combine to give an estimated peak power out of the oscillator of 37 kW (assuming a factor of 0.88 for sech^2 pulse shapes). At this peak power, this laser surpasses many commercial free-space OPA systems and becomes attractive for laser surgery of human tissue, for industrial materials modification, and for driving broadband coherent supercontinua in the mid-infrared.

Since fundamental mode locking occurs at a relatively low pump power, we investigated the soliton dynamics for higher pump values. In the near-infrared, there have been many reports of multiple pulsing observed in soliton lasers at high pump powers [19–21]. This phenomenon has its origin in the peak-power-limiting feature of the soliton circulating in the laser cavity [19]. When additional pump power is applied above the single-soliton level, the extra laser power initially goes into the dispersive wave in the cavity. However, once the power increases to a level in which the cavity could support a second soliton, a second soliton arises and circulates within the cavity at a delay relative to the first soliton pulse. The delay between the various solitons and their relative intensities depends on the linear cavity phase delay [19]. To test for the existence of this multiple-soliton state in this laser system, we employed a long time-base, background-free autocorrelation capable of a temporal measurement window ± 28 ps.

By increasing the pump power (and thus the pulse energy), the fundamental soliton decreases its pulse duration in accordance with the soliton area theorem until the gain bandwidth starts to limit the pulsewidth [21]. At a sufficiently high pump power, a portion of the background dispersive-wave radiation can experience a large enough intensity fluctuation to initiate shaping by the saturable absorber and evolve into an ultrashort pulse. The middle panel of Fig. 5 shows two trailing pulses arising in this manner (launched pump power = 3.5 W). This process continues repeatedly as the pump power is increased. Indeed, in many near-infrared soliton fiber lasers one can sequentially create or annihilate circulating solitons one at a time in the cavity by carefully adjusting the pump power. As can be seen in Fig. 5, the solitons are closely trailing the fundamental soliton in time and thus experience less gain due to the slow gain recovery time in holmium ($t_{\text{rec}} \sim \mu\text{s}-\text{ms}$ for rare-earth gain media) [21,22]. If the secondary pulses arise sufficiently far away in time from the fundamental soliton, they can experience the full gain of the laser medium and grow to be identical to the original circulating soliton.

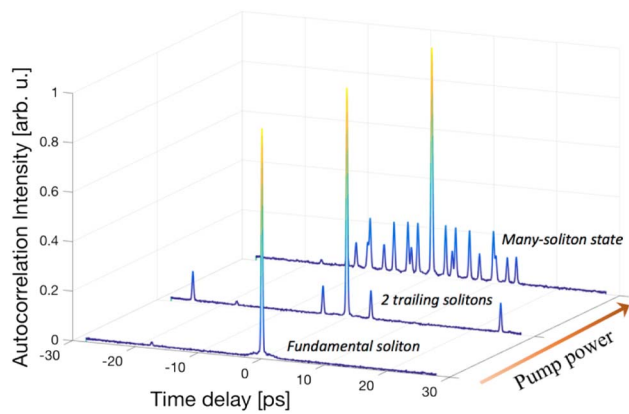


Fig. 5. Long time-base, background-free autocorrelation of the laser as a function of pump power. At high pump power, many solitons are supported. Reducing the pump power systematically eliminates solitons until only the fundamental soliton remains. Due to the symmetry of the autocorrelation, the trailing pulses are also mirrored on the leading side.

At even higher pump power (3.8 W launched), the pulse train splits into a many-soliton state, where the cavity supports as many as nine extra solitons. As shown in Fig. 5 (top curve), there appear to be overlapping solitons as well. This could be an indication of bound-state solitons in the laser cavity [21]. In this high-pump-power, multi-pulse state, the laser emits an average power of >400 mW. This measurement confirms the existence in the mid-infrared of the well-known multiple-soliton effect that has previously been observed in near-infrared fiber lasers.

In summary, we have shown that by using holmium-doped ZBLAN fiber in conjunction with NPR-based mode locking, a record 37 kW peak power pulses can be produced. The roughly 100 nm central emission redshift of the transition of holmium relative to erbium means that the laser operates in the mid-infrared water vapor window located near 2.9 μm . Although this is a relatively small shift compared to the absolute wavelength, the water vapor lines decrease drastically in strength beyond 2.8 μm . This fact allows us to achieve a pulse duration of 180 fs and a bandwidth of 60 nm, which represents, to the best of our knowledge, the highest performance reported to date from ultrafast mid-infrared fiber lasers. Long-range, free-space atmospheric propagation is now more likely, while at the same time, the central emission wavelength is closer to the absorption peak of liquid water ($\alpha_{2876} \approx 2\alpha_{2800}$). These parameters are vital to applications in laser surgery. Finally, we investigated the soliton phenomenon of multiple pulsing in the mid-infrared using a long time-base autocorrelation. We showed that beyond the fundamental mode-locked state, multiple pulse formation is possible, and we observed initial evidence for bound-state soliton pairs.

In future work, we will investigate amplifying this laser to even higher power. A benefit of these systems relative to other mid-infrared laser sources is that they are ideal for amplification

in an external cavity fiber amplifier. The diffraction-limited beam and commensurate core size of the mid-infrared fiber amplifier should allow for highly efficient amplification to the multi-100-kW peak power level. At these power levels and with the sub-200-fs pulse duration, we should be able to drive a broadband, coherent supercontinuum using chalcogenide-based nonlinear fibers. The creation of coherent octave-spanning supercontinua in this system would open the door for these fiber lasers to be used as frequency combs in the mid-infrared wavelength region.

Funding. Air Force Office of Scientific Research (AFOSR) (FA2386-16-1-4030); Australian Research Council (ARC) (DP140101336).

Acknowledgment. We thank Nathan Kutz from the University of Washington for helpful insight into multiple pulse formation in soliton laser cavities. We thank Tomonori Hu from Miriad Technologies for useful discussions and help with the experimental setup. This material is based upon work supported by the AFOSR.

REFERENCES

1. T. Hu, S. Jackson, and D. Hudson, *Opt. Lett.* **40**, 4226 (2015).
2. S. Duval, M. Bernier, V. Fortin, J. Genest, M. Piché, and R. Vallée, *Optica* **2**, 623 (2015).
3. S. Duval, M. Olivier, V. Fortin, M. Bernier, M. Piché, and R. Vallée, *Proc. SPIE* **9728**, 972802 (2016).
4. F. Adler, P. Masłowski, A. Foltynowicz, K. Cossel, T. Briles, I. Hartl, and J. Ye, *Opt. Express* **18**, 21861 (2010).
5. M. Cizmeciyan, H. Cankaya, A. Kurt, and A. Sennaroglu, *Opt. Lett.* **34**, 3056 (2009).
6. A. Griffith, R. Lau, J. Cardenas, Y. Okawachi, A. Mohanty, R. Fain, Y. Lee, M. Yu, C. Phare, C. Poitras, A. Gaeta, and M. Lipson, *Nat. Commun.* **6**, 6299 (2015).
7. C. Wang and P. Sahay, *Sensors* **9**, 8230 (2009).
8. J. Mandon, G. Guelachvili, and N. Picqué, *Nat. Photonics* **3**, 99 (2009).
9. J.-L. Boulnois, *Lasers Med. Sci.* **1**, 47 (1986).
10. D. Hudson, *Opt. Fiber Technol.* **20**, 631 (2014).
11. T. Hu, D. Hudson, and S. Jackson, *Opt. Lett.* **39**, 2133 (2014).
12. X. Zhu and N. Peyghambarian, *Adv. Optoelectron.* **2010**, 501956 (2010).
13. P. Golding, S. Jackson, T. King, and M. Pollnau, *Phys. Rev. B* **62**, 856 (2000).
14. H. Zhang, H. Xiao, P. Zhou, X. Wang, and X. Xu, *IEEE Photonics J.* **5**, 1501706 (2013).
15. S. Jackson, F. Bugge, and G. Erbert, *Opt. Lett.* **32**, 3349 (2007).
16. A. Librantz, S. Jackson, F. Jagosich, L. Gomes, G. Poirier, S. Ribero, and Y. Messaddeq, *J. Appl. Phys.* **101**, 123111 (2007).
17. S. Antipov, M. Ams, R. Williams, E. Magi, M. Withford, and A. Fuerbach, *Opt. Express* **24**, 30 (2016).
18. S. Kelly, K. Smith, K. Blow, and N. Doran, *Opt. Lett.* **16**, 1337 (1991).
19. D. Tang, L. Zhao, B. Zhao, and A. Liu, *Phys. Rev. A* **72**, 043816 (2005).
20. F. Li, P. Wai, and J. N. Kutz, *J. Opt. Soc. Am. B* **27**, 2068 (2010).
21. J. Kutz, B. Collings, K. Bergman, and W. Knox, *IEEE J. Quantum Electron.* **34**, 1749 (1998).
22. E. Desurvire, *IEEE Photon. Technol. Lett.* **1**, 196 (1989).